ACS Medicinal Chemistry Letters

Letter

pubs.acs.org/acsmedchemlett

Discovery of PF-04449913, a Potent and Orally Bioavailable Inhibitor of Smoothened

Michael J. Munchhof,*,† Qifang Li,‡ Andrei Shavnya,‡ Gary V. Borzillo,‡ Tracey L. Boyden,‡ Christopher S. Jones,§ Susan D. LaGreca,∥ Luis Martinez-Alsina,‡ Nandini Patel,‡ Kathleen Pelletier,‡ Larry A. Reiter,⊥ Michael D. Robbins,# and George T. Tkalcevic‡

†Michael J. Munchhof LLC, 266 West Road, Salem, Connecticut 06420, United States

‡Pfizer Global Research and Development, Groton, Connecticut 06340, United States

§24 Queen Eleanor Drive, Gales Ferry, Connecticut 06335, United States

∥INC Research, Old Lyme, Connecticut 06371, United States

⊥Reiter.MedChem, 32 West Mystic Avenue, Mystic, Connecticut 06355, United States

#Bristol-Meyers Squibb, Princeton, New Jersey 08540, United States

Supporting Information

ABSTRACT: Inhibitors of the Hedgehog signaling pathway have generated a great deal of interest in the oncology area due to the mounting evidence of their potential to provide promising therapeutic options for patients. Herein, we describe the discovery strategy to overcome the issues inherent in lead structure **1** that resulted in the identification of Smoothened inhibitor 1-((2*R*,4*R*)-2-(1*H*-benzo[*d*]imidazol-2-yl)-1-methylpiperidin-4-yl)-3-(4-cyanophenyl)urea (PF-04449913, **26**), which has been advanced to human clinical studies.

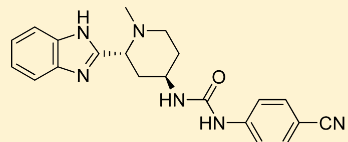

PF-04449913 (26)

KEYWORDS: *Smoothened, Hedgehog signaling pathway, PF-04449913*

The Hedgehog (Hh) signaling pathway has generated a great deal of interest in the oncology community due to emerging evidence of its importance in a broad range of cancers, including basal cell carcinoma, bladder, colorectal, leukemias, lung, medulloblastoma, pancreatic, prostate, and stomach.[1] The Hh signaling cascade is activated by binding of one of three Hh ligands, Sonic Hedgehog (Shh), Indian Hedgehog (Ihh), or Desert Hedgehog (Dhh), to their receptor Patched (Ptch).[2] This leads to the activation of Smo, a 7-transmembrane protein, by relieving Ptch's suppressive effect on Smo, triggering a cascade that results in the activation of three transcription factors, Gli1, Gli2, and Gli3, leading to proliferation. Hh signaling is critical in tissue patterning in early development, homeostasis, and tissue regeneration. Deregulation of the pathway via mutations or autocrine or paracrine mechanisms of ligand overexpression leads to hyperproliferative conditions.[1]

Over a decade ago, Beachy reported the first Smo antagonist, cyclopamine (Figure 1).[3] Cyclopamine was isolated from the corn lilly, *Veratrum californicum*, by Richard Keeler and co-workers in 1964.[4] Beachy showed that cyclopamine interacted directly with Smo by incorporating photoaffinity and fluorescent labels.[5] Subsequent work with cyclopamine and its derivatives provided the tools needed to demonstrate the importance of Smo signaling in the Hh pathway and in preclinical tumor growth inhibition models.[6] From these studies, Smo emerged as an attractive target in the Hh signaling pathway for pharmacological intervention. Several research groups have reported the advancement of Smo inhibitors into clinical trials, including Infinity's IPI 926, Novartis's NVP-LDE225 and Genentech's GDC-0449 (vismodegib).[7,8] The published clinical results on the latter compound and a recent New Drug Application (NDA) filing with the FDA are

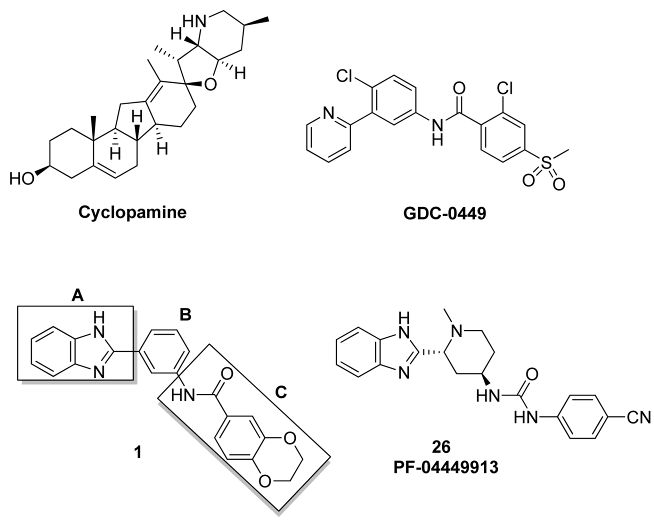

Figure 1.

Received: October 14, 2011
Accepted: December 13, 2011
Published: December 21, 2011

Scheme 1. Synthesis of 8[a]

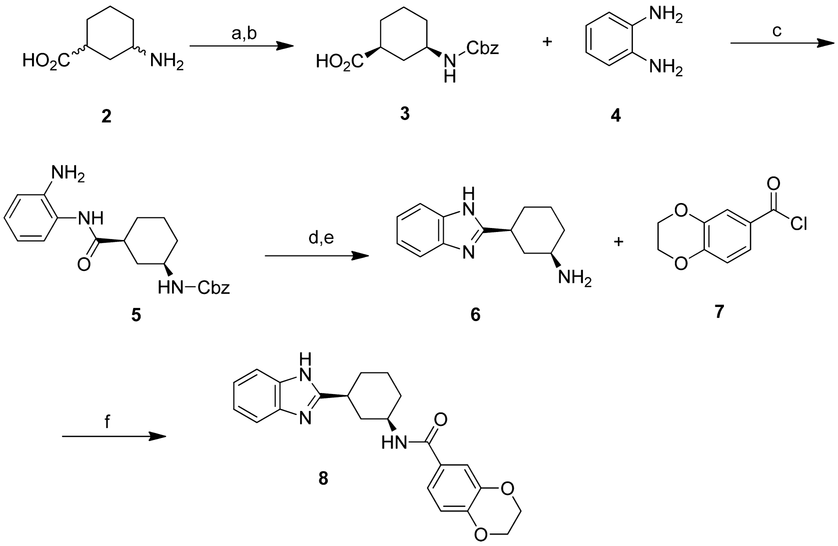

[a]Reagents and conditions: (a) Benzyl chloroformate, sodium carbonate, dioxane, H_2O. (b) Chiral chromatography,[18] 33% (two steps). (c) Isobutyl chloroformate, triethylamine, CH_2Cl_2. (d) Glacial acetic acid at 100 °C, 45% (two steps). (e) Hydrogen, 10% palladium on activated carbon, methanol, 95%. (f) Triethylamine, THF, and H_2O, 83%.

Table 1. In Vitro Pharmacology Data for 1, 8, and 15

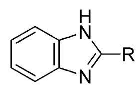

Entry	Structure	Gli-luciferase reporter reporter in C3H10T1/2 (IC_{50}) (nM)	Fold loss in activity relative to **1**	cLogD @ pH 6.5
1	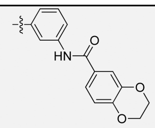	5		4.48
8	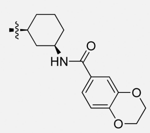	88	18	2.85
15	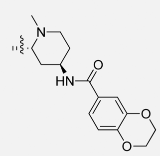	43	9	1.06

encouraging and support the pursuit of Smo antagonists for the treatment of cancer.[9]

Concurrently with Beachy's reports on cyclopamine, additional chemically distinct classes of Smo inhibitors began to appear in the literature from this group and others.[10−12] Benzimidazoles, represented by compound **1**,[13] were one of the more chemically attractive motifs in that they were low molecular weight, potent, and lacked reactive and chemically unstable functionality. While **1** has excellent potency, it suffered from poor metabolic stability (human in vitro free CLint = 314 μL/min/kg)[14,15] and high plasma protein binding across species (<1% free) that can be attributed to its high lipophilicity (cLog *D* at pH 6.5 = 4.48). Additionally, its aqueous solubility was low (0.1 μg/mL). These issues presented significant challenges for further development of compounds from this series. On the basis of these data, design strategies were pursued to decrease the lipophilicity, improve hepatic clearance, increase free fraction, and enhance solubility.[16] Results of the efforts leading to the discovery of PF-04449913, 1-((2*R*,4*R*)-2-(1*H*-benzo[*d*]imidazol-2-yl)-1-methylpiperidin-4-yl)-3-(4-cyanophenyl)urea **26**, are described herein.

Initially, compound **1** was divided into three fragments: benzimidazole (**A**), phenyl (**B**), and aminoacylaryl (**C**) groups, for structure−activity exploration purposes (Figure 1). At the outset, our strategy focused on replacing the central phenyl ring **B**. The phenyl group contributed a significant amount of lipophilicity, and it was important to understand if this lipophilicity was counterbalanced by a commensurate increase in potency. Additionally, it was critical to understand the role of **B** as a scaffold for the proper spatial arrangement of the **A** and **C** substituents. An attractive option to test this was to replace the phenyl ring with cyclohexyl, since the *cis*-1,3-substituted configuration would place the substituents in similar vectors as **1**. Additionally, the target was synthetically readily accessible allowing for a rapid testing of the above hypothesis.

Scheme 1 details the synthesis of *N*-((1*R*, 3*S*)-3-(1*H*-benzo[*d*]imidazol-2-yl)cyclohexyl]-2,3-dihydrobenzo[*b*][1,4]-dioxine-6-carboxamide **8**. The amino group of commercially available 3-aminocyclohexanecarboxylic acid (**2**)[17] was protected as the carbobenzoxy derivative, and the mixture was separated by chiral HPLC affording (1*S*,3*R*)-3-(benzyloxycarbonylamino)cyclohexanecarboxylic acid (**3**).[18] Conversion of the carboxylic acid to the mixed anhydride and coupling with benzene 1,2-diamine afforded amide **5**, which was then stirred in glacial acetic acid at 100 °C for 2 h to form the benzimidazole. Deprotection and acylation with 3-dihydrobenzo-[*b*][1,4]dioxine-6-carbonyl chloride completed the synthesis of **8**. The remaining diastereomers were prepared in an analogous manner.

The (1*R*,3*S*)-isomer (**8**) emerged as the most potent diastereomer following screening in the Gli-luciferase reporter

Scheme 2. Synthesis of 15[a]

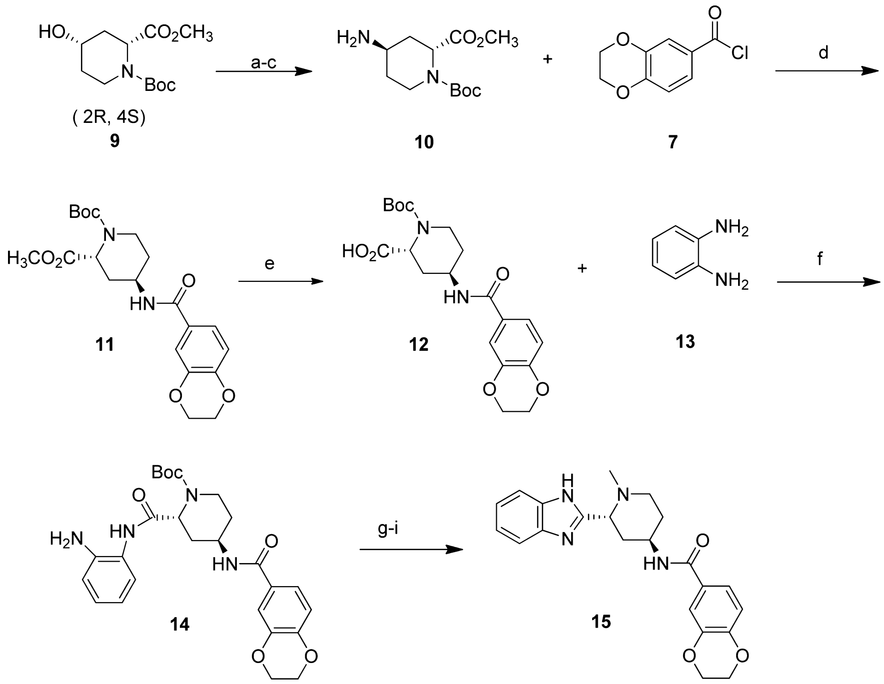

[a]Reagents and conditions: (a–c) MsCl, dimethylaminopyridine, pyridine then sodium azide, THF then Pd/C, methanol 97% for three steps di-*tert*-butyl dicarbonate, THF, H_2O, 97%. (d) Pyridine, THF. (e) LiOH, THF/H_2O/methanol 96% for two steps. (f) Benzotriazole-1-yl-oxy-tris-(dimethylamino)-phosphonium hexafluorophosphate, diisopropylethylamine, DMF, 80%. (g–i) Acetic acid at 65 °C, then trifluoroacetic acid, then 37% formaldehyde, H_2O, sodium cyanoborohydride in THF 78% for three steps.

Scheme 3. Synthesis of Amino Piperidine Intermediate 20[a]

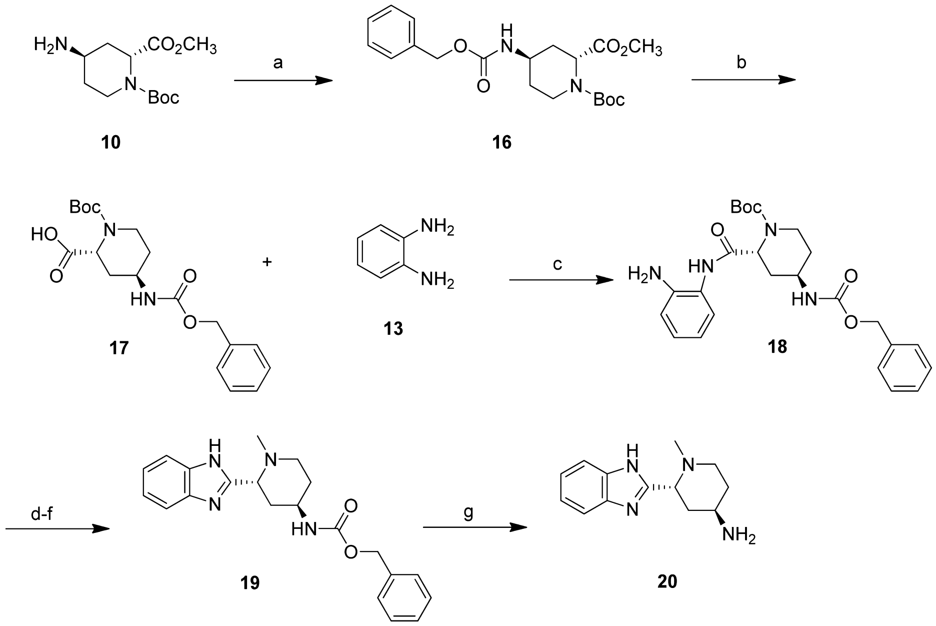

[a]Reagents and conditions: (a) Benzylchloroformate, triethylamine, dioxane, 0 °C, 92%. (b) LiCl, THF/H_2O/methanol, 95%. (c) Benzotriazole-1-yl-oxy-tris-(dimethylamino)-phosphonium hexafluorophosphate, diisopropylethylamine, DMF, 65%. (d–f) Acetic acid at 65 °C then trifluoroacetic acid then 37% formaldehyde, H_2O, sodium cyanoborohydride in THF, 76%. (g) Pd/C, H_2, MeOH, 98%.

assay, being about 18-fold less potent than **1** (Table 1).[19] In addition to the structural insight gained with the cyclohexyl replacement, an additional advantage was that it reduced the calculated lipophilicity by 1.6 units (cLog *D* at pH 6.5 = 2.85) relative to **1**. This increase in polarity translated into improved in vitro metabolic stability, with no turnover observed in human microsomes and moderate clearance in rat (33 mL/min/kg).[20] In vivo pharmacokinetic studies in rats demonstrated a good correlation between the in vitro predicted clearance and the observed in vivo measured clearance, indicating that **8** was primary cleared by hepatic oxidation. However, the oral bioavailability of **8** was only 4%,[21] despite excellent permeability

Table 2. In Vitro Pharmacology Data for Ureas (21−28)

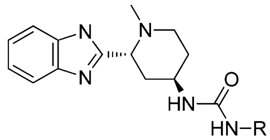

Entry	R	Gli-luciferase reporter reporter in C3H10T1/2 (IC_{50}) (nM)	cLogD@ pH 6.5	Human Liver Microsomal CLint (μL/min/kg)	Human Liver Microsomal freeCLint (μL/min/kg)
21	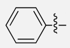	103	1.82	< 7.60	< 9.60
22	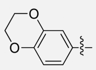	45	1.62	< 7.60	< 12.0
23	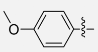	35	1.48	17.9	23.9
24	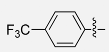	5	3.18	21.3	68.9
25	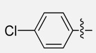	20	3.06	25.4	38.7
26	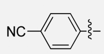	5	2.06	< 12.8	< 19.8
27	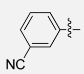	72	2.24	NT	NT
28	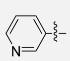	191	1.64	29.4	31.7

as measured in a Caco-2 assay,[22] with no *p*-glycoprotein-mediated efflux observed. Together, these data led us to conclude that poor solubility was likely responsible for the poor oral absorption. Solubility measurements showed that, although the solubility was improved over **1** (37 vs 0.1 μg/mL), it was still poor. Even though potency was improved by modifications to the **A** and **C** regions of **8**, all attempts to improve solubility by introducing polar or ionizable groups in these areas of the molecule led to losses in potency, stalling the progression of the series.

Having exhausted options in the other regions of **8**, attention was turned to the cyclohexyl core. Amine-containing heterocyclic alkyl groups, such as pyrrolidines and piperidines, offered an alternative strategy to enhance solubility. Depending on the substitution pattern, the potential existed to design compounds with a basic amine in the core of the pharmacophore. This would allow for the preparation of salts with a variety of counterions, with the potential to improve solubility.[23]

Preparation and profiling of several piperidine and pyrrolidine cores led to a focus on the 1,2,4 substituted piperidines, *N*-[(2-(1*H*-benzimidazol-2-yl)-1-methylpiperidin-4-yl]-2,3-dihydro-1,4-benzodioxine-6-carboxamides, due to the promising potency observed with the 2*R*,4*R*-diastereoisomer

Table 3. Summary of Properties of PF-04449913 (26)

MW	374
cLog *P*, cLog *D*	2.28, 2.06
measured Log *D*	2.48
polar surface area (Å^2)	97
microsomal CLi (mL/min/kg)	
rat ($f_{ub,mic}$ 0.57)	67
dog ($f_{ub,mic}$ 0.54)	<14
human ($f_{ub,mic}$ 0.61)	6.3
cytochrome P450 IC_{50} values (1A2, 2C8, 2C9, 2C19, 2D6, 3A4)	all >30 μM
pK_a	6
solubility of di-HCl monohydrate salt	
H_2O	0.02 mg/mL
pH 6.5 PBS	1.15 mg/mL
pH 1.2 SGN	>69 mg/mL
protein binding (% free, f_u)	
rat	10.9
dog	14.1
human	9.1
permeability (Caco-2, P_{app} cm/s)	
AB	5.98×10^{-6}
BA	15.6×10^{-6}
Genetox	
Ames assay	negative
micronucleus assay	negative

in vivo pharmacokinetics				
	CL (mL/min/kg)	V_{ss}	$t_{1/2}$ (h)	*F* (%)
rat	31	4.8	1.4	33
dog	3.9	4.3	2.9	68

15. Piperidine **15** was prepared as shown in Scheme 2. Commercially available (2*R*,4*S*)-1-*tert*-butyl 2-methyl 4-hydroxypiperidine-1,2-dicarboxylate (**9**) was converted to the mesylate that was displaced with sodium azide. Reduction of the azide and acylation with 3-dihydrobenzo-[*b*][1,4]dioxine-6-carbonyl chloride (**7**) afforded **11**. Hydrolysis of the ester, activation, and coupling with 1,2-diaminobenzene gave **14**, which was treated with acetic acid, forming the benzimidazole ring. Deprotection of the N-1 amine of the piperidine and reductive amination with formaldehyde completed the synthesis of **15**. The remaining diastereomers were obtained in an analogous manner by starting with the appropriate 1-*tert*-butyl 2-methyl 4-hydroxypiperidine-1,2-dicarboxylate.

Piperidine **15** was about 2-fold more potent than **8** (Table 1), with the other diastereomers being 4 to >50-fold less potent than **8**. While **15** was stable in rat and human microsomes, it was cleared rapidly in vivo (Clp > 70 mL/min/kg) in rats.[24] In dogs, the clearance was moderate (Clp = 18 mL/min/kg) and correlated well with the in vitro microsomal prediction (Clint = 19 mL/min/kg). The bioavailability of **15**, following oral dosing in dog, was 33% and, after accounting for the moderate clearance, indicated that greater than 50% of the dose was absorbed.[25]

To further improve the potency and in vivo pharmacokinetic properties of **15**, a systematic effort was undertaken focusing on (1) optimization of the substituent on the N-1 piperidine nitrogen, (2) understanding the affects of substitution on the benzimidazole ring, (3) identification of the optimal group on the 4-aminopiperidine, and (4) extensive profiling of compounds in in vivo pharmacokinetic studies. Efforts to balance potency and pharmacokinetic properties were met with limited success in the first two areas. Ultimately, it was exploration of replacements for the 2,3-dihydrobenzo[*b*][1,4]-dioxine-6-carboxy group on the 4-amino piperidine that proved most productive.

Structure−activity relationships in the 4-aminopiperidine region of **15** were rapidly explored using parallel synthesis methods employing amine **20** (Scheme 3). Amine **20** was prepared from (2*R*,4*R*)-1-*tert*-butyl 2-methyl 4-aminopiperidine-1,2-dicarboxylate **10**. Protection of the 4-amino group as the carbobenzoxy derivative and hydrolysis of the ester afforded **17**. Activation of the acid, coupling to 1,2-diaminobenzene (**13**), and cyclization were carried out in an analogous manner as described in Scheme 2. Reductive removal of the carbobenzoxy protecting group gave **20**. Amine **20** was coupled with a diverse set of carboxylic acids and isocyanates in high yields using standard conditions. Although potency gains were difficult to achieve in the amide series, the urea exploration proved to be more productive. Following preparation of a small set of alkyl, cyclic alkyl, and aryl ureas, phenyl urea **21** was identified as an attractive lead for further investigation (Table 2). Further studies to optimize the potency of **21** provided the following general trends: (1) *ortho* substitution was not tolerated; (2) both *meta* (**27**) and *para* (**23−26**) substitution generally increased potency, with *para* being preferred (**26** vs **27**); (3) replacement of phenyl with pyridyl diminished potency (**28**), as did additional heteroaromatic replacements; and (4) methylation of either of the urea nitrogen's produced inactive compounds.

Profiling of several ureas both in vitro and in vivo revealed that *p*-cyano urea **26** comprised the best overall combination of properties.[26] The physical properties and in vitro and in vivo pharmacokinetic data for **26** are summarized in Table 3. In vitro microsomal assays predicted **26** to have high clearance in rat and low clearance in dog and human, with free fractions in rat, dog, and human plasma of 10−14%. Additionally, **26** did not inhibit any of the major cytochrome P450 isoforms, nor did it form covalent adducts when incubated with glutathione, either with or without metabolic activation. It is negative in Ames and micronucleus assays used to assess genotoxicity risk. The aqueous solubility of the dihydrochloride salt is poor; however, solubility in simulated gastric fluid is high. Permeability is moderate in Caco-2 cells with asymmetry, indicating that **26** is a *p*-glycoprotein substrate. In vivo pharmacokinetic studies in rat[27] and dog[28] demonstrated that the in vivo clearances correlated well with in vitro microsomal data, and volumes of distribution were moderate, with oral bioavailabilities of 33 and 68%, in rat and dog, respectively. Together, on the basis of the preclinical in vitro and in vivo pharmacokinetic data, **26** was predicted to have low plasma clearance (1.03 mL/min/kg), moderate volume of distribution (2.7 L/kg), a half-life of 30 h, and an oral bioavailability of 55% in humans.

In summary, PF-04449913 (**26**), a Smoothened inhibitor was identified possessing excellent potency and physical properties that translate to an attractive predicted human pharmacokinetic profile. On the basis of these data, **26** was advanced to in vivo tumor growth inhibition studies, preclinical safety studies, and ultimately to human clinical trials. These results will be reported in separate disclosures.

■ ASSOCIATED CONTENT

Supporting Information

Experimental details for the preparation and characterization of **8**, **15**, **20−22**, and **26−28** and methods for in vitro profiling. This material is available free of charge via the Internet at http://pubs.acs.org.

■ AUTHOR INFORMATION

Corresponding Author

*Tel: 860-287-5924. E-mail: mikemunchhof@yahoo.com.

Notes

The authors declare no competing financial interest.

■ REFERENCES

(1) Heretsch, P.; Tzagkaroulaki, L.; Giannis, A. Modulators of the hedgehog signaling pathway. *Bioorg. Med. Chem.* **2010**, *18*, 6613−6624.

(2) Rubin, L. L.; de Sauvage, F. Targeting the Hedgehog pathway in cancer. *Nat. Rev. Drug Discovery* **2006**, *5*, 1026−1033.

(3) Taipale, J.; Chen, J. K.; Cooper, M. K.; Wang, B.; Mann, R. K.; Milenkovic, L.; Scott, M. P.; Beachy, P. A. Effects of oncogenic mutations in Smoothened and Patched can be reversed by cyclopamine. *Nature* **2000**, *406*, 1005−1009.

(4) Keeler, R. F.; Binns, W. Chemical compounds of Veratrum californicum related to congenital ovine cyclopian malformations. Extraction of active material. *Proc. Soc. Exp. Biol. Med.* **1964**, *116*, 123−127.

(5) Chen, J. K.; Taipale, J.; Cooper, M. K.; Beachy, P. A. Inhibition of Hedgehog signaling by direct binding to Smoothened. *Genes Dev.* **2002**, *16*, 2743−2748.

(6) Jiang, J.; Hui, C.-c. Hedgehog Signaling in Development and Cancer. *Dev. Cell* **2008**, *15*, 801−812.

(7) Peukert, S.; Miller-Moslin, K. Small-Molecule Inhibitors of the Hedgehog Signaling Pathway as Cancer Therapeutics. *ChemMedChem* **2010**, *5*, 500−512.

(8) Pan, W.; Wu, X.; Jiang, J.; Gao, W.; Wan, Y.; Cheng, D.; Han, D.; Liu, J.; Englund, N. P.; Wang, Y.; Peukert, S.; Miller-Moslin, K.; Yaun, J.; Guo, R.; Matsumoto, M.; Vattay, A.; Jiang, Y.; Tsao, J.; Fangxian, S.; Pferdekamper, A. C.; Dodd, S.; Tuntland, T.; Wieslawa, M.; Kelleher, J. F.; Yao, Y.; Warmuth, M.; Williams, J.; Dorsch, M. Discovery of NVP-LDE225, a Potent and Selective Smoothened Antagonist. *ACS Med. Chem. Lett* **2010**, *1* (3), 130−134.

(9) Doggrell, S. A. The hedgehog pathway inhibitor GDC-0449 shows potential in skin and other cancers. *Expert Opin. Invest. Drugs* **2010**, *19*, 451−454.

(10) Chen, J. K.; Taipale, J.; Young, K. E.; Maiti, T.; Beachy, P. A. Small molecule modulation of Smoothened activity. *Proc. Natl. Acad. Sci. U.S.A.* **2002**, *99*, 14071−14076.

(11) Beachy, P. A.; Chen, J. K.; Taipale, A. J. N. Modulators of hedgehog signaling pathways, compositions and uses related thereto. WO 2003088970, 2003.

(12) Frank-Kamenetsky, M.; Zhang, X. M.; Bottega, S.; Guicherit, O.; Wichterle, H.; Dudek, H.; Bumcrot, D.; Wang, F. Y.; Jones, S.; Shulok, J.; Rubin, L. L.; Porter, J. A. Small-molecule modulators of Hedgehog signaling: identification and characterization of Smoothened agonists and antagonists. *J. Biol.*, **2002**, *1*, Article 10.

(13) Rubin, L.; Guicherit, O. M.; Price, S.; Boyd, E. A. Mediators of Hedgehog Signaling Pathways, Compositions and uses related thereto. WO2003011219, 2003.

(14) Free CL_{int} = CL_{int}/fuMic.

(15) Obach, R. S. Prediction of human clearance of twenty-nine drugs from hepatic microsomal intrinsic clearance data: An examination of in vitro half-life approach and nonspecific binding in microsomes. *Drug Metab. Dispos.* **1999**, *27*, 1350−1359.

(16) Hughes, J. D.; Blagg, J.; Price, D. A.; Bailey, S.; DeCrescenzo, G. A.; Devraj, R. V.; Ellsworth, E.; Fobian, Y. M.; Gibbs, M. E.; Gilles, R. W.; Greene, N.; Huang, E.; Krieger-Burke, T.; Loesel, J.; Wager, T.;

Whiteley, L.; Zhang, Y. Physiochemical Drug Properties Associated With In Vivo Toxicological Outcomes. *Bioorg. Med. Chem. Lett.* **2008**, *18*, 4872−4875.
(17) The *cis/trans* mixture of stereoisomers was used.
(18) Chiralcel OJ-H 3 cm × 25 cm, eluting with 20% of methanol in carbon dioxide.
(19) The remaining diastereomers were 50 to >500-fold less active than **1**.
(20) IV dosing formulation, 2 mg/kg in 20% PEG400/80% H_2O, Clp = 25 mL/min/kg.
(21) Oral dosing formulation, 5 mg/kg in 0.5% methylcellulose in water.
(22) Caco-2 AB P_{app} 85 × 10^{-6} cm/s, BA P_{app} 65 × 10^{-6} cm/s.
(23) Serajuddin, A. T. M. Salt formation to improve drug solubility. *Adv. Drug Delivery Rev.* **2007**, *59*, 603−616.
(24) Subsequent experiments to understand this disconnect were not conclusive. Less than 5% of parent drug concentrations was detected in bile and urine.
(25) Oral dosing formulation, 5 mg/kg in 0.5% methylcellulose in water.
(26) Genentech's GDC-0449 was tested in the Gli-Luciferase assay and had an IC_{50} of 5 nM. This provided a means of calibrating the relative in vitro potency of **26** to GDC-0449 in this assay.
(27) IV dosing formulation, 1 mg/kg 10% EtOH/20% PEG400/70% PBS in solution. Oral dosing formulation, 1 mg/kg methylcellulose in water.
(28) IV dosing formulation, 0.5 mg/kg 10% EtOH/20% PEG400/70% PBS in solution. Oral dosing formulation, 3 mg/kg methylcellulose in water.